THE JOURNAL OF BIOLOGICAL CHEMISTRY VOL. 285, NO. 45, pp. 35104–35112, November 5, 2010

Carbon Flow of Heliobacteria Is Related More to *Clostridia* than to the Green Sulfur Bacteria*[S]

Received for publication, July 14, 2010, and in revised form, August 30, 2010 Published, JBC Papers in Press, August 31, 2010, DOI 10.1074/jbc.M110.163303

Kuo-Hsiang Tang[‡§1,2], Xueyang Feng[¶1], Wei-Qin Zhuang[‖], Lisa Alvarez-Cohen[‖], Robert E. Blankenship[‡§], and Yinjie J. Tang[¶3]

From the Departments of [‡]Biology, [§]Chemistry, and [¶]Energy, Environment, and Chemical Engineering, Washington University, St. Louis, Missouri 63130 and the [‖]Department of Civil and Environmental Engineering, University of California, Berkeley, California 94720

The recently discovered heliobacteria are the only Gram-positive photosynthetic bacteria that have been cultured. One of the unique features of heliobacteria is that they have properties of both the photosynthetic green sulfur bacteria (containing the type I reaction center) and *Clostridia* (forming heat-resistant endospores). Most of the previous studies of heliobacteria, which are strict anaerobes and have the simplest known photosynthetic apparatus, have focused on energy and electron transfer processes. It has been assumed that like green sulfur bacteria, the major carbon flow in heliobacteria is through the (incomplete) reductive (reverse) tricarboxylic acid cycle, whereas the lack of CO_2-enhanced growth has not been understood. Here, we report studies to fill the knowledge gap of heliobacterial carbon metabolism. We confirm that the CO_2-anaplerotic pathway is active during phototrophic growth and that isoleucine is mainly synthesized from the citramalate pathway. Furthermore, to our surprise, our results suggest that the oxidative (forward) TCA cycle is operative and more active than the previously reported reductive (reverse) tricarboxylic acid cycle. Both isotopomer analysis and activity assays suggest that citrate is produced by a putative (*Re*)-citrate synthase and then enters the oxidative (forward) TCA cycle. Moreover, in contrast to (*Si*)-citrate synthase, (*Re*)-citrate synthase produces a different isomer of 2-fluorocitrate that is not expected to inhibit the activity of aconitase.

Heliobacteria are a relatively newly discovered group of anaerobic photosynthetic bacteria. All of the cultured heliobacteria require organic carbon for anoxygenic growth, and several of the species can fix nitrogen (1, 2). Heliobacteria are the only cultured Gram-positive photosynthetic bacteria and are phylogenetically related to the bacterial phylum *Firmicutes*, such as the aerobic *Bacillus* and anaerobic *Clostridia* (1). Among 10 cultured heliobacteria (2), *Heliobacterium modesticaldum* is the only one that can grow at temperatures of >50 °C. Madigan and co-workers (1, 3) reported that pyruvate, lactate, acetate (+HCO_3^-), or yeast extract can support the phototrophic growth of *H. modesticaldum*, and our recent studies demonstrated that D-sugars can also support the growth of *H. modesticaldum* (4).

An unusual feature of heliobacteria is that they have properties of both green sulfur bacteria (containing the type I reaction center) and *Clostridia* (forming heat-resistant endospores) (1). Heliobacteria have the simplest photosynthetic apparatus among the photosynthetic organisms (5), and most of the research on them has been focused on understanding the photosynthetic machinery and energy transfer processes (1, 6–8). In contrast, our knowledge of phototrophic carbon metabolism by heliobacteria is still poorly developed.

Only two reported studies have experimentally probed the carbon metabolism of heliobacteria; one is our recent study with *H. modesticaldum* (4), and the other is the 1994 report by Kelly and co-workers (9) on *Heliobacterium* strain HY-3. Our studies highlighted the critical roles that pyruvate plays during phototrophic and chemotrophic growth of *H. modesticaldum*, reported on three new carbon sources for *H. modesticaldum*, and verified the genomic information. Kelly and co-workers (9) assayed activity for the enzymes in the TCA cycle and employed ^{13}C NMR to analyze ^{13}C-labeled protein-based amino acids using [2-^{13}C]pyruvate or [2-^{13}C]acetate. Furthermore, the genes *aclAB*, encoding ATP citrate lyase (ACL),[4] and *gltA*, encoding citrate synthase (CS), have not been annotated in the *H. modesticaldum* genome (5), and neither we (4) nor Kelly and co-workers (9) detected the enzymatic activities for ACL or CS. Together, previous studies suggested that the RTCA cycle is not complete in *H. modesticaldum* (Fig. 1*A*) (4, 5) and *Heliobacterium* strain HY-3 (9).

Note that ^{13}C NMR may be insufficient for generating complete labeling information of key metabolites, as ^{13}C NMR cannot directly detect labeled carbon on the carboxyl group of an amino acid if its α-carbon is not labeled (10). More importantly, essential questions remain unresolved for carbon metabolism of heliobacteria. (*a*) If the (incomplete) RTCA cycle is employed

* This work was supported by National Science Foundation Career Grant MCB0954016 (to Y. J. T.) and Exobiology Program of NASA Grant NNX08AP62G (to R. E. B.).

[S] The on-line version of this article (available at http://www.jbc.org) contains supplemental Tables S1–S5, Fig. S1, and additional references.

[1] Both authors contributed equally to this work.

[2] To whom correspondence may be addressed: Depts. of Biology and Chemistry, Campus Box 1137, Washington University, St. Louis, MO 63130. Tel.: 314-935-6343; Fax: 314-935-4432; E-mail: j.tang@wustl.edu.

[3] To whom correspondence may be addressed: Dept. of Energy, Environment, and Chemical Engineering, Campus Box 1180, Washington University, St. Louis, MO 63130. Tel.: 510-295-5651; Fax: 314-935-5464; E-mail: yinjie.tang@seas.wustl.edu.

[4] The abbreviations used are: ACL, ATP citrate lyase; CS, citrate synthase; FAc, fluoroacetate; 2-FC, 2-fluorocitrate; α-KG, α-ketoglutarate; OAA, oxaloacetate; OTCA cycle, oxidative (forward) TCA cycle; PEP, phosphoenolpyruvate; RTCA cycle, reductive (reverse) TCA cycle; BChl *g*, bacteriochlorophyll *g*; 8^1-OH-Chl a_F, 8^1-hydroxychlorophyll *a* with a farnesol tail.

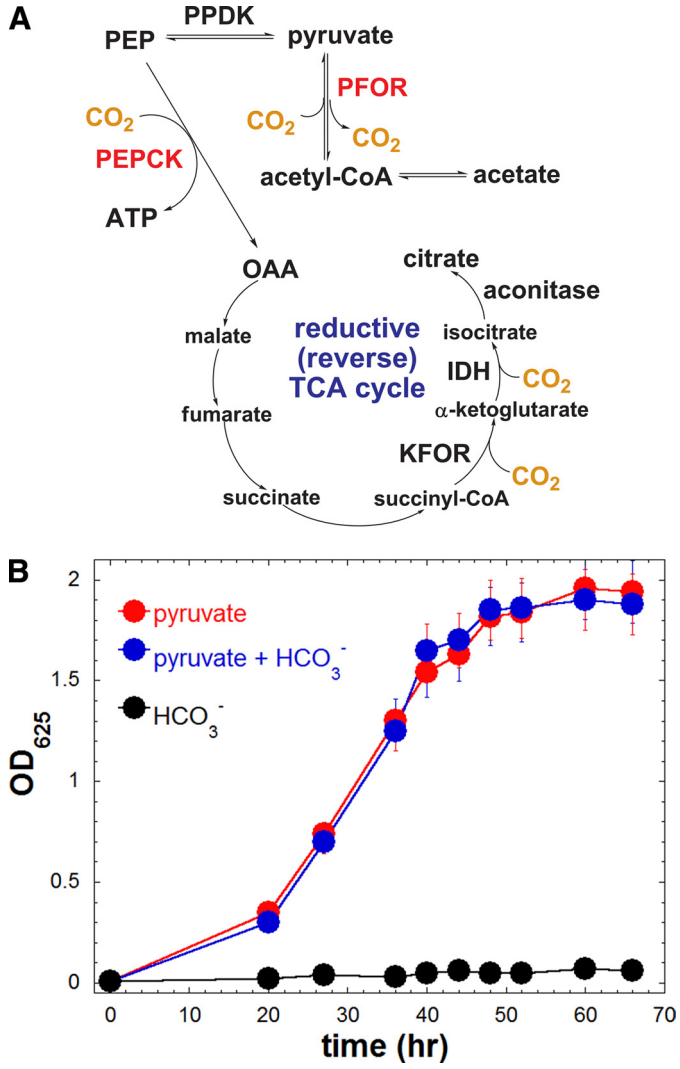

FIGURE 1. *A*, previously proposed carbon flow in *H. modesticaldum* from genomic information and enzymatic activity assays. *B*, phototrophic growth curve of *H. modesticaldum* grown on pyruvate, HCO_3^-, or pyruvate and HCO_3^- as the defined carbon source. Cell density was estimated by measuring the optical density (*OD*) at 625 nm (see the "Experimental Procedures"). *PFOR*, pyruvate:ferredoxin oxidoreductase; *PEPCK*, phosphoenolpyruvate carboxykinase; *KFOR*, α-KG:ferredoxin oxidoreductase; *IDH*, isocitrate dehydrogenase.

for biomass production in heliobacteria (Fig. 1*A*), then CO_2 is essential for phototrophic growth (a metabolic type similar to the green sulfur bacteria that employ an RTCA cycle) (11). However, no apparent CO_2-enhanced growth has been observed for pyruvate-grown heliobacterial cultures. (*b*) Some ^{13}C-labeled patterns in the study by Kelly and co-workers (9) suggested that the oxidative (forward) TCA (OTCA) cycle is operative. If this is the case, it is difficult to understand how the OTCA cycle could possibly be initiated without the encoding genes or enzymatic activities of ACL or CS.

This study is intended to apply both biochemical methods and ^{13}C-based metabolite analysis via mass spectrometry to address those essential questions by investigating how the TCA cycle and amino acid biosynthesis are performed by *H. modesticaldum*. Our results identify the missing link for the carbon metabolism of *H. modesticaldum* (and perhaps *Heliobacterium* strain HY-3) and suggest that the carbon flow of *H. modesticaldum* is more akin to *Clostridia* than to the green sulfur bacteria.

EXPERIMENTAL PROCEDURES

Materials—Chemicals and enzymes were obtained from Sigma. The ^{13}C-labeled sodium bicarbonate, [1-^{13}C]- and [3-^{13}C]pyruvate were obtained from Cambridge Isotope Laboratories, Inc. The DNA oligomers were obtained from Integrated DNA Technology without further purification.

Cell Cultures—The cell cultures employed in this study are listed below. Cell density was estimated by measuring the optical density (OD) of a suspension of cells at 625 nm (OD_{625}) for the cell growth of both *H. modesticaldum* and *Roseobacter denitrificans* because absorbance of photosynthetic pigments is minimal around 625 nm (4), and OD_{600} was measured to estimate the growth of *Desulfovibrio vulgaris* Hildenborough (DvH), in which no photosynthetic pigment was present. Autoclaved subcultures were used as negative controls, and all of the experiments were performed in triplicate.

H. modesticaldum—The *H. modesticaldum* strain Ice1^T culture was provided by Dr. Michael T. Madigan (Southern Illinois University, Carbondale) and was grown phototrophically in a minimal medium (1, 4) with pyruvate (20 mM) and (±)HCO_3^- (20 mM) as the carbon sources. The fresh medium was inoculated with 1–2% cell culture in the late exponential growth phase. Physiological studies with fluoroacetate (FAc) for the pyruvate-grown cultures were performed with 20 mM pyruvate and 20 mM FAc included in the growth medium. The cultures were grown inside the anaerobic chamber (Coy) in low intensity light (100 ± 10 μmol/m^2/s) at 46–48 °C.

R. denitrificans—The *R. denitrificans* OCh114 culture, obtained from Dr. J. T. Beatty (University of British Columbia, Vancouver, Canada), was grown aerobically in a defined medium with pyruvate (20 mM), FAc (20 mM), or pyruvate (20 mM) + FAc (20 mM) as the sole carbon sources. The defined growth medium was prepared as reported (12). The cultures were grown at 28 °C (20–30%-filled Erlenmeyer flask) with shaking at 150 rpm in the dark.

D. vulgaris Hildenborough (DvH)—DvH was kindly provided by Dr. Terry C. Hazen (Lawrence Berkeley National Laboratory, Berkeley, CA). DvH was grown in a defined growth medium containing (per liter) NaCl (1.0 g), $MgCl_2 \cdot 6H_2O$ (0.5 g), KH_2PO_4 (0.2 g), NH_4Cl (0.3 g), KCl (0.3 g), $CaCl_2 \cdot 2H_2O$ (0.015 g), $MgSO_4 \cdot 7H_2O$ (0.2 g), a trace element solution (1 ml) (13), a Na_2SeO_3/Na_2WO_4 solution (1 ml) (14), resazurin (10 mg), lactate (5 mM), Na_2SO_4 (5 mM), and with a N_2/CO_2 (80:20, v/v) headspace. After autoclaving and cooling to room temperature, the medium was supplied with a vitamin mixture solution (0.5 ml) (15). DvH was subcultured into fresh medium in triplicate with 1% (v/v) inoculate, and cell cultures were grown at 30 °C anaerobically. FAc amended cultures were prepared in the same content except FAc (1.5 mM) was added before inoculation.

RNA Extraction and Quantitative Real Time PCR—The transcriptomic profiling data were generated using the approaches described elsewhere (16). The primer sequences for QRT-PCR are listed in supplemental Table S1.

Isotopomer Analysis via GC-MS—The isotopomer analysis was performed using the methods reported previously (17) and is described in the supplemental material.

Activity Assays for Citrate Synthase—Enzymatic activities were performed in triplicate with cell-free extracts that were prepared using the procedure as described earlier (4). Protein concentration in cell extracts was determined by the Bradford assay (18) using bovine serum albumin as the standard. The reaction turnover for the reaction catalyzed by CS was followed by the formation of 5,5′-dithiobis-2-nitrobenzoic acid or Ellman's reagent-modified CoA using the method reported previously (9, 19) with minor modification. To minimize oxygen in the assay mixture for measuring CS activity, all of the reagents (5,5′-dithiobis-2-nitrobenzoic acid, metal ions), substrates (acetyl-CoA, oxaloacetate), and buffer were prepared with oxygen-free water in an anaerobic chamber (Coy), and the assay components were mixed in a tightly sealed cuvette inside the anaerobic chamber prior to removal for the spectral measurements. The reaction was initiated by the addition of oxaloacetate (OAA) (0.5 mM), and the increase at A_{412} was followed to monitor the activity. The amount of CoA production was estimated using a standard calibration curve with β-mercaptoethanol. The control experiment was performed with the same procedure with water rather than OAA added to initiate the reaction.

RESULTS

Carbon Metabolism in H. modesticaldum

In this study, we probed the central carbon metabolic pathway with the following approaches: (i) physiological studies with fluoroacetate; (ii) isotopomer data; (iii) mass spectrum of photosynthetic pigments; and (iv) transcriptomic profiles. Pyruvate is the best known organic carbon source for supporting the phototrophic growth of *H. modesticaldum* (3, 4) and several other heliobacteria (1), and it was used for probing the carbon metabolism of *H. modesticaldum*.

Physiological Studies with Fluoroacetate—FAc has been reported as a metabolic toxin. The toxicity of FAc is generally recognized to arise from the fact that the carbon flow in the OTCA cycle is blocked through the inhibition of aconitase by (−)-*erythro*-(2*R*,3*R*)-2-F-citrate (2-FC), which is synthesized from F-acetyl-CoA and OAA by CS (20). Consistent with this hypothesis, an aerobic anoxygenic photoheterotrophic bacterium *R. denitrificans*, which has been known to have an active OTCA cycle (12), was notably inhibited by FAc (Fig. 2*A*). In contrast, the growth of *H. modesticaldum* on pyruvate was similar with FAc *versus* without FAc (Fig. 2*B*). It is known that FAc, an acetate analog, can be taken up by *H. modesticaldum* and converted into F-acetyl-CoA, because the *acsA* gene, encoding acetyl-CoA synthetase (ACS), has been annotated and the enzymatic activity of ACS has been reported (4). Furthermore, acetate ($+HCO_3^-$) is also known to support the phototrophic growth of *H. modesticaldum* (1, 3, 4). Consistent with the physiological studies, the transcript levels of genes for carbon metabolism are similar (within ~2 $\Delta\Delta C_T$) for cultures grown on pyruvate (20 mM) and with or without the addition of FAc (20 mM) (Table 1). Together, our studies indicate little effect of

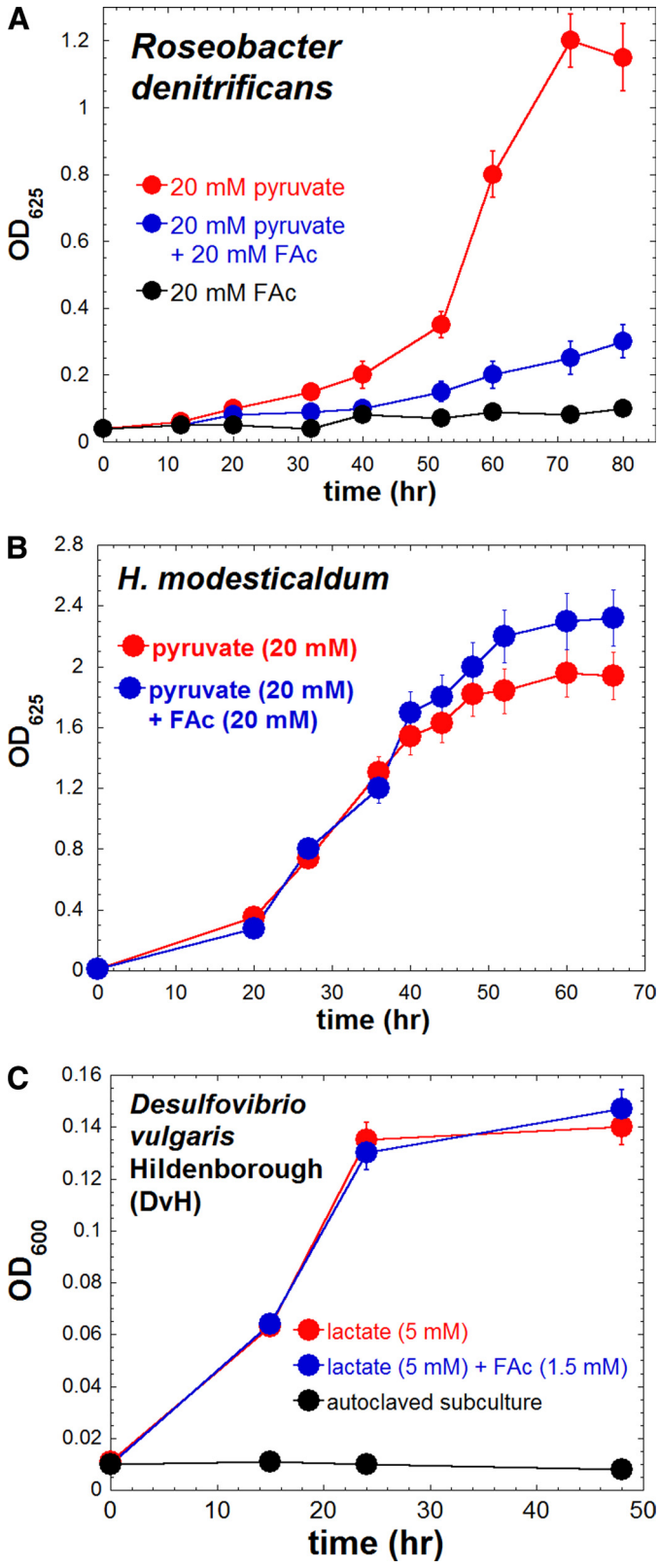

FIGURE 2. **Effect of FAc for the growth of *R. denitrificans*, *H. modesticaldum*, and *D. vulgaris* Hildenborough (*DvH*).** *A*, growth curve of *R. denitrificans* grown on pyruvate, FAc, or pyruvate and FAc as the carbon source; *B*, growth curve of *H. modesticaldum* during photoheterotrophic growth on pyruvate with or without FAc; *C*, growth curve of DvH grown on lactate with or without FAc.

TABLE 1

The transcript level of the genes for carbon metabolism of *H. modesticaldum* during photoheterotrophic growth on pyruvate with or without FAc

The genes encoding the enzymes in the (R)TCA cycle are highlighted in boldface italic.

Gene	ΔC_T[a] (pyruvate)	ΔC_T[a] (pyruvate + FAc)	$\Delta\Delta C_T$ (ΔC_T in pyruvate − ΔC_T in pyruvate + FAc)	relative expression level (pyruvate vs. pyruvate + FAc) = $2^{\Delta\Delta C_T}$
pykA (HM1_0076, pyruvate kinase)	11.0 ± 0.2	12.7 ± 0.2	1.7 ± 0.4	3.2 ± 1.3
acn (HM1_0105, aconitase)	10.7 ± 0.1	12.6 ± 0.1	1.8 ± 0.2	3.5 ± 1.1
fdxR (HM1_0289, Fd-NADP$^+$ reductase, FNR)	12.2 ± 0.0	14.2 ± 0.1	2.0 ± 0.1	4.0 ± 1.0
porA (HM1_0807, pyruvate, Fd oxidoreductase, PFOR)	9.8 ± 0.2	11.7 ± 0.1	1.8 ± 0.3	3.5 ± 1.2
acsA (HM1_0951, acetyl-CoA synthetase)	12.1 ± 0.0	14.3 ± 0.2	2.1 ± 0.2	4.3 ± 1.1
icd (HM1_1471, isocitrate dehydrogenase)	10.7 ± 0.2	12.4 ± 0.0	1.6 ± 0.2	3.0 ± 1.1
mdh (HM1_1472, malate dehydrogenase	10.9 ± 0.0	12.4 ± 0.0	1.5 ± 0.0	2.8 ± 0.0
ackA (HM1_2157, acetate kinase)	11.6 ± 0.1	13.6 ± 0.0	2.0 ± 0.1	4.0 ± 1.0
ppdK (HM1_2461, pyruvate phosphate dikinase)	11.3 ± 0.1	13.2 ± 0.1	1.9 ± 0.2	3.7 ± 1.1
korC (HM1_2762, KFOR, γ subunit)	9.9 ± 0.0	10.8 ± 0.2	0.9 ± 0.2	1.9 ± 1.1
oorB (HM1_2763, KFOR, β subunit)	9.2 ± 0.0	10.9 ± 0.1	1.7 ± 0.1	3.2 ± 1.0
korA (HM1_2766, KFOR, α subunit)	8.9 ± 0.1	10.7 ± 0.0	1.8 ± 0.1	3.5 ± 1.0
korD (HM1_2767, KFOR, δ subunit)	8.9 ± 0.0	11.0 ± 0.1	2.1 ± 0.1	4.3 ± 1.0
nifV (HM1_0858, homocitrate synthase)	15.0 ± 0.1	15.4 ± 0.2	0.4 ± 0.3	1.3 ± 1.2
aksA (HM1_2993, homocitrate synthase)	10.5 ± 0.2	12.0 ± 0.2	1.5 ± 0.4	2.8 ± 1.3
pckA (HM1_2773, PEP carboxykinase)	11.9 ± 0.0	13.5 ± 0.1	1.6 ± 0.1	3.0 ± 1.0

[a] $\Delta C_T = C_T$ (the threshold cycle) of the target gene $- C_T$ of the 16 S rRNA gene.

FAc on the growth of *H. modesticaldum*, implying that (−)-*erythro*-2-FC cannot be synthesized in *H. modesticaldum*, in agreement with the findings that no genes encoding CS and ACL have been annotated in the genome (5), and no enzymatic activities of CS or ACL have been detected for *H. modesticaldum* (4).

Moreover, when the anaerobic sulfate-reducing bacterium *D. vulgaris* Hildenborough (DvH) was grown with a 1:1 molar ratio of [2-^{13}C]acetate and nonlabeled lactate, significant amounts of labeled carbon were detected in the biomass (supplemental Table S2), indicating that DvH can utilize acetate for producing biomass. Furthermore, isotopomer analysis using [2-^{13}C]acetate (supplemental Table S2) and a previous DvH flux analysis (21) indicate that acetate ↔ acetyl-CoA is reversible in DvH. No FAc inhibition was detected during the growth of DvH (Fig. 2*C*).

Isotopomer Analysis by GC-MS—Previous studies have established that the cell growth of *H. modesticaldum* is best supported by pyruvate (1, 3, 4). We used ^{13}C-labeled pyruvate and characterized the protein-based amino acids for probing the central carbon metabolic pathways. *H. modesticaldum* is recognized as a photoheterotrophic bacterium (3, 4), and CO_2 neither supports nor enhances its phototrophic growth (Fig. 1*B*). When *H. modesticaldum* was grown on [1-^{13}C]pyruvate, aspartate was mainly double-labeled, and glutamate was primarily single-labeled (Table 2). In the (incomplete) RTCA cycle (Fig. 1), α-KG, the precursor of glutamate, is synthesized from OAA, the precursor of aspartate, which results in the incorporation of all the carbons from aspartate into the carbon backbones of glutamate. Also, assuming that some of the CO_2 molecules assimilated through the RTCA cycle are $^{13}CO_2$ generated from the reaction [1-^{13}C]pyruvate + CoA → acetyl-CoA + $^{13}CO_2$ (Fig. 1), ^{13}C-labeled content is expected to be higher for glutamate than for aspartate. Consequently, the multiply labeled instead of the singly labeled glutamate would eventually become dominant through the (incomplete) RTCA cycle. However, in this study, the observed lower ^{13}C-labeled content of glutamate compared with aspartate with [1-^{13}C]pyruvate-grown cells cannot have been generated by cells utilizing solely the (incomplete) RTCA cycle. Furthermore, the carbon flux of *H. modesticaldum* cannot primarily go through the (incomplete) RTCA cycle but must instead mainly transform via the OTCA cycle. Moreover, aspartate was dominantly single-labeled (M1 >0.8), and glutamate was mostly double-labeled (M2 >0.75) for cells using [3-^{13}C]pyruvate (supplemental Table S3), in agreement with significant carbon flow through the OTCA cycle.

Mass Spectrum of Photosynthetic Pigments—We further analyzed the mass spectrum of BChls we reported earlier using MALDI-TOF (matrix-assisted laser desorption ionization time-of-flight) mass spectrometry (4), in which ^{13}C-labeled photosynthetic pigments (bacteriochlorophyll *g* (BChl *g*) and 8^1-hydroxychlorophyll *a* with a farnesol tail (8^1-OH-Chl a_F)) were detected using [3-^{13}C]pyruvate. Both BChl *g* and 8^1-OH-Chl a_F were synthesized from eight molecules of glutamate and eight molecules of acetyl-CoA (for generating the farnesyl tail with a 15-carbon unit at C17^3 position), and thus ^{13}C-labeled BChl *g* and 8^1-OH-Chl a_F are expected using [3-^{13}C]pyruvate. The *m*/*e* for BChl *g* and 8^1-OH-Chl a_F is 796.7 and 812.7, respectively, with unlabeled pyruvate, and for BChl *g* and 8^1-OH-Chl a_F is 816.8 and 832.8, respectively, with [3-^{13}C]pyruvate. The number of labeled carbons for the labeled BChl *g* or 8^1-OH-Chl a_F was estimated to be 21–22 using the program IsoPro 3.1. Using [3-^{13}C]pyruvate as the carbon source, glutamate is expected to be double-labeled through the OTCA cycle because citrate is double-labeled via condensation of [3-^{13}C]OAA and [2-^{13}C]acetyl-CoA, where glutamate is single-labeled through the RTCA cycle (from [3-^{13}C]OAA). Thus, 16 carbons are labeled through the RTCA cycle (eight single-labeled glutamates and eight single-labeled acetyl-CoAs) and 24-labeled carbons through the OTCA cycle (eight double-labeled glutamates and eight single-labeled acetyl-CoAs) using [3-^{13}C]pyruvate. Thus, observations of higher ^{13}C contents on BChl *g* and 8^1-OH-Chl a_F in the mass spectrum than expected from the RTCA cycle would suggest that the OTCA cycle contributes to the formation of glutamate and α-KG. Consistent with this hypothesis, glutamate was found to be mostly double-

TABLE 2
Isotopomer labeling patterns of protein-based amino acids in the cultures grown on [1-^{13}C]pyruvate

Amino acid	Precursor	Ion[a]	M-57[b]	M-159[c]	f302[d]	Proposed ^{13}C-enriched positions (shown as asterisk)
Ala	Pyruvate	M0	0.20	0.85	0.20	C-C-*COOH
		M1	0.77	0.09	0.79	
		M2	0.03	0.06	0.01	
Gly	Serine	M0	0.24	0.98	0.12	C-*COOH
		M1	0.75	0.02	0.48	
		M2	0.01		0.40	
Val	Pyruvate	M0	0.20	0.89	0.28	C-C-C-C-*COOH
		M1	0.77	0.09	0.72	
		M2	0.03	0.01	0.00	
Leu	Pyruvate	M0	0.60	0.83	0.63	Nonlabeled
	Acetyl-CoA	M1	0.36	0.14	0.36	
		M2	0.03	0.02	0.01	
		M3	0.00	0.00		
Ile	Pyruvate	M0	0.66	0.83	0.69	Nonlabeled
	Threonine	M1	0.25	0.16	0.25	
		M2	0.08	0.01	0.06	
		M3	0.01	0.00		
Met	Aspartate	M0	0.09	0.22	0.17	C-S-*C-C-C-*COOH
	Methyl-THF[e]	M1	0.24	0.58	0.51	
		M2	0.51	0.20	0.32	
		M3	0.15	0.01		
Ser	3-Phosphoglycerate	M0	0.19	0.94	0.21	C-C-*COOH
		M1	0.77	0.06	0.78	
		M2	0.04	0.00	0.01	
Thr	Aspartate	M0	0.11	0.26	0.11	*C-C-C-*COOH
		M1	0.29	0.72	0.46	
		M2	0.59	0.02	0.43	
Phe	PEP	M0	0.08	0.13	0.22	C-C-*C-*C-C-C-C-C-*COOH
	Erythrose 4-phosphate	M1	0.11	0.29	0.77	
		M2	0.31	0.53	0.01	
		M3	0.46	0.04		
		M4	0.04	0.01		
Asp	OAA	M0	0.11	0.27	0.27	*COOH-C-C-*COOH
		M1	0.31	0.71	0.73	
		M2	0.56	0.01	0.01	
Glu	α-Ketoglutarate	M0	0.26	0.28	0.82	C-C-C-C-*COOH
		M1	0.64	0.68	0.18	
		M2	0.09	0.04	0.00	
		M3	0.01	0.00		
His	Ribose 5-phosphate	M0	0.13	0.13	0.92	N-C-N-C-*C-*C-C-COOH
		M1	0.41	0.41	0.06	
		M2	0.32	0.34	0.02	
		M3	0.10	0.07		
Lys	Aspartate	M0	0.14	0.28	0.92	C-C-*C-C-C-*COOH
	Pyruvate	M1	0.26	0.68	0.08	
		M2	0.58	0.03	0.00	
		M3	0.02	0.00		
		M4	0.00	0.00		

[a] M0, M1, M2, M3, and M4 indicate mass fraction of the unlabeled, single-labeled, double-labeled, triple-labeled, and quadruple-labeled amino acid.
[b] $[M-57]^+$ indicates un-fragmented amino acid detected by GC-MS.
[c] $[M-159]^+$ indicates an amino acid minus the α−carboxyl group detected by GC-MS.
[d] f302 is the fragment of the first two carbons in a derivatized amino acid (17).
[e] THF is tetrahydrofolate.

labeled (M2 >75%) using [3-^{13}C]pyruvate (supplemental Table S3).

Transcriptomic Profiles—All of the genes encoding the enzymes in the RTCA cycle, except for ACL, have been annotated in the *H. modesticaldum* genome (5). Table 1 shows that genes in the RTCA cycle (highlighted in **boldface italic**) are expressed and that the transcript level for the genes responsible for carbon metabolism is similar (at most a 4-fold difference) in the pyruvate-grown cultures with and without FAc.

Taking all of the experimental evidence together, our studies indicate that in addition to the incomplete RTCA cycle, the OTCA cycle is also employed by *H. modesticaldum*. Like the RTCA cycle, the OTCA cycle is not complete but mainly contributes to the formation of α-KG, as indicated by isotopomer analysis and mass spectrometry of photosynthetic pigments. The active OTCA cycle is consistent with the observed lack of CO_2-enhanced pyruvate growth of *H. modesticaldum* (Fig. 1*B*), because CO_2 is produced through the OTCA cycle.

Citrate Synthase Activity Detected Anaerobically

Table 2 shows that over 50% aspartate and 60% glutamate were labeled in the β-carboxyl group with [1-^{13}C]pyruvate as the carbon source, implying that citrate formation is possibly catalyzed by (*Re*)-citrate synthase ((*Re*)-CS) (Fig. 3). Both (*Re*)-CS and normal CS (*i.e.* (*Si*)-CS) catalyze the formation of citrate through aldol condensation of OAA and acetyl-CoA, whereas the acetyl-CoA moiety is added to the "pro-*R*" and "pro-*S*" arm of citrate through catalysis of (*Re*)-CS and (*Si*)-CS, respectively (Fig. 3).

We have previously showed that no CoA production was detected with acetyl-CoA and OAA added in the cell extracts of *H. modesticaldum* under aerobic conditions and without diva-

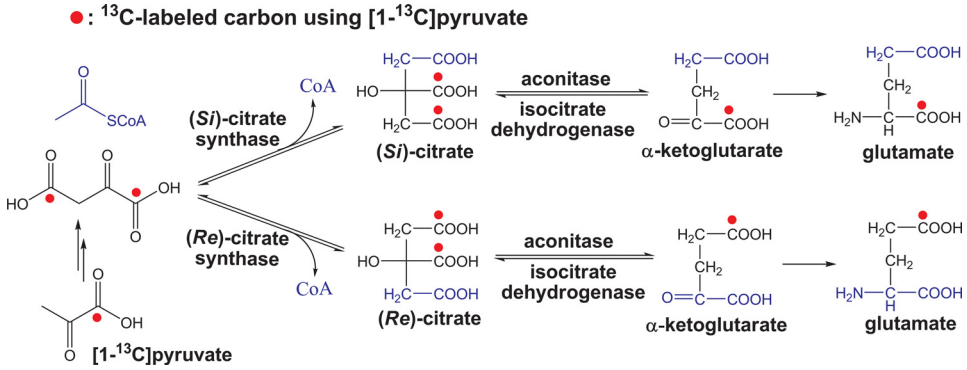

FIGURE 3. **Reactions catalyzed by the (*Re*)- *versus* (*Si*)-citrate synthase, aconitase, and isocitrate dehydrogenase.** ^{13}C labeling distributions in citrate, α-ketoglutarate, and glutamate using [1-^{13}C]pyruvate are shown.

lent metal ion supplied, confirming that (*Si*)-CS is not produced by *H. modesticaldum* (4). Anaerobic conditions have not been reported to be required for the activity of (*Si*)-CS. To test if citrate can be produced by *H. modesticaldum* via the catalysis of (*Re*)-CS, rigorous efforts were made to minimize the oxygen content in the assay mixtures (described under "Experimental Procedures"), because oxygen-sensitive and divalent metal ion (Mn^{2+}, Mg^{2+}, or Co^{2+}) dependences were reported for the activity measurements of (*Re*)-CS (19). The increase of A_{412} for 5,5′-dithiobis-2-nitrobenzoic acid-modified CoA can be detected with Mn^{2+}, OAA, and acetyl-CoA under anaerobic conditions, suggesting the presence of the CS activity in *H. modesticaldum*. The catalytic activity of the novel CS, likely (*Re*)-CS, was estimated to be 50 ± 20 nmol/min/mg protein.

Anaplerotic-CO_2 Fixation Pathways

The isotopomer labeling experiment with ^{13}C-labeled HCO_3^- and unlabeled pyruvate as the carbon source showed that over 50% alanine was labeled (supplemental Table S4) and that all the labeled alanine was labeled at the carboxyl group. The labeling pattern suggests that the reaction catalyzed by pyruvate:ferredoxin oxidoreductase (acetyl-CoA + CO_2 + $2Fd_{red}$ + $2H^+$ ↔ pyruvate + CoA + $2Fd_{ox}$) is freely reversible and very active so that the labeled bicarbonate is incorporated into pyruvate. The isotopomer analysis is in agreement with our recent physiological studies that pyruvate:ferredoxin oxidoreductase plays a central role in carbon metabolism of *H. modesticaldum* (4). Moreover, when using [1-^{13}C]pyruvate as the carbon source, aspartate can be synthesized either from the CO_2-anaplerotic pathways with pyruvate and/or phosphoenolpyruvate (PEP) and $^{13}CO_2$ (from decarboxylation of [1-^{13}C]pyruvate), leading to double-labeled aspartate, or through the OTCA cycle, in which aspartate is not expected to be double labeled. The predominance of double-labeled aspartate indicates the high carbon flow via the CO_2-anaplerotic pathway and low flux from the OTCA cycle, consistent with observed activity of PEP carboxykinase illustrated in our recent studies (4), and confirming that the OTCA cycle is not complete as genes encoding the enzymes specific for the OTCA cycle have not been annotated in the genome (5).

Amino Acid Biosynthesis

The isotopomer analysis for biosynthesis of several amino acids is illustrated as follows.

Alternative Isoleucine Biosynthesis Pathway—Isoleucine is typically synthesized through the threonine pathway (Fig. 4). Using [1-^{13}C]pyruvate as the carbon source, threonine was mainly double-labeled (M2 >58%), so isoleucine would be expected to be double-labeled via the threonine pathway. Table 2 shows that isoleucine was largely nonlabeled (M0 >60%) with [1-^{13}C]pyruvate, suggesting that isoleucine was mostly synthesized through the citramalate pathway, although all of the genes in the threonine pathway have been annotated. In the citramalate pathway, citramalate synthase (CimA) catalyzes the formation of D-*erythro*-3-methylmalate (*i.e.* citramalate) through condensation of pyruvate and acetyl-CoA (Fig. 4). Two gene loci, HM1_1519 and HM1_1515, encoding putative CimA in the citramalate pathway have been annotated in the genome. The amino acid sequence encoding by gene locus HM1_1519 shows >50% identity to the recently reported CimA (Teth514_1204) in *Thermoanaerobacter* sp. X514 (22), which is a close relative to the genus *Clostridium*. The supplemental Table S5 lists the bacteria with the citramalate pathway identified.

Normal Pathways for Alanine, Serine, Phenylalanine, and Lysine Biosynthesis—The isotopomer pattern suggested alanine and serine are synthesized from pyruvate and PEP, respectively. Also, using [3-^{13}C]pyruvate as the carbon source, the labeling pattern in supplemental Table S3 indicates that phenylalanine is synthesized from the common biosynthetic pathway with erythrose 4-phosphate and PEP as precursors in agreement with the genomic information (5). Furthermore, Pickett *et al.* (9) also reported the same results regarding pathways of alanine, serine, and phenylalanine biosynthesis for *Heliobacterium* strain HY-3.

The labeling patterns of lysine in the isotopomer analysis suggest that lysine is synthesized through the common diaminopimelate pathway with pyruvate and aspartate as the precursors, rather than through the α-amino adipate pathway (supplemental Fig. S1), in which 2-ketoglutarate and acetyl-CoA are condensed and converted to lysine. This conclusion is consistent with the fact that all genes in the α-aminoadipate pathway are missing, except for the genes encoding putative homocitrate synthase (*nifV* (HM1_0858) and *aksA* (HM1_2993)). This enzyme catalyzes the formation of homocitrate ((*R*)-2-hydroxybutane-1,2,4-tricarboxylate) by condensing α-KG and acetyl-CoA. Note that the *askA* gene is expressed with higher transcript level (Table 1). The possible function of the homocitrate synthase for carbon metabolism will be discussed later.

DISCUSSION

Growth of H. modesticaldum with FAc

Fig. 2 shows that there is no detectable difference in the growth of *H. modesticaldum* with or without FAc, suggesting that (−)-*erythro*-2-FC cannot be synthesized by CS or/and ACL

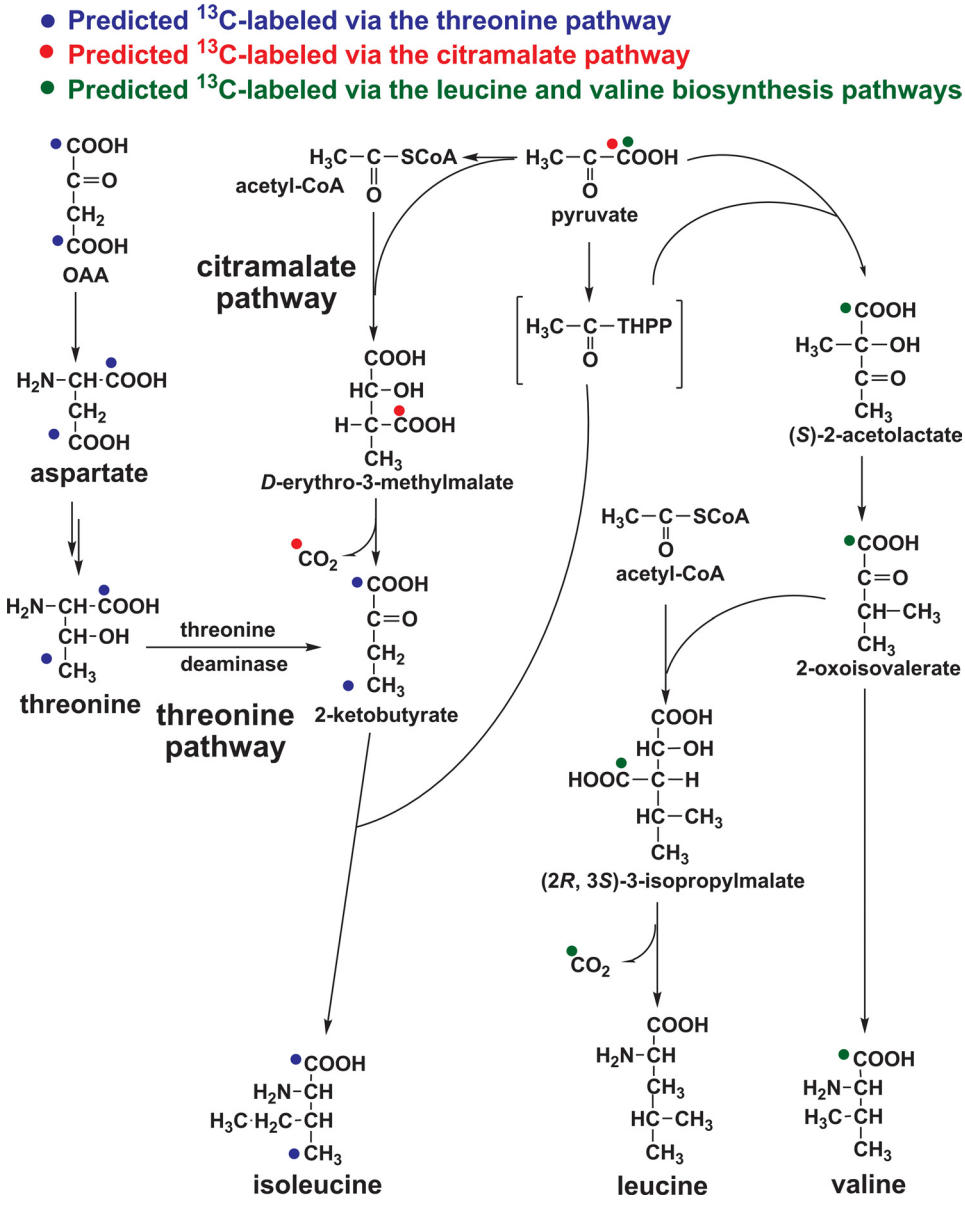

FIGURE 4. **Proposed biosynthesis pathways for isoleucine, including the citramalate and threonine pathways, leucine, and valine.** Predicted ^{13}C labeling distributions using [1-^{13}C]pyruvate are shown.

in *H. modesticaldum*. However, the lack of genes encoding ACL and CS along with the lack of the enzymatic activities is inconsistent with our presented isotopomer data, which suggest that at least a partial OTCA cycle is active and an oxygen-sensitive novel CS is produced by *H. modesticaldum* to initiate the OTCA cycle. If a novel CS is produced by *H. modesticaldum*, then the lack of FAc inhibition during the growth of *H. modesticaldum* needs to be explained. Two working hypotheses can be considered.

High Flux from Pyruvate to Acetyl-CoA to Compete with F-acetyl-CoA—Similar activity of F-acetyl-CoA *versus* acetyl-CoA for normal CS has been reported previously (23). Assuming that (−)-*erythro*-2-FC is synthesized by a putative novel CS, acetyl-CoA from pyruvate could compete with F-acetyl-CoA from FAc for the interactions of the putative CS. A high flux from pyruvate to acetyl-CoA is suggested from our recent studies showing that conversion of pyruvate to acetyl-CoA, catalyzed by pyruvate:ferredoxin oxidoreductase, is very active in pyruvate-grown *H. modesticaldum* (4) and the isotopomer data presented in this report. However, Fig. 2*A* shows that the pyruvate-grown *R. denitrificans*, which is also known to exhibit high flux from pyruvate to acetyl-CoA (12), was notably reduced by the presence of FAc, suggesting that other factors must contribute to the lack of FAc-inhibition on the phototrophic growth of *H. modesticaldum*.

Different Stereoisomer of 2-FC Is Synthesized—Alternatively, it is possible that the putative CS catalyzes the formation of a 2-FC isomer other than (−)-*erythro*-2-FC. Note that only one of four possible 2-FC isomers, (−)-*erythro*-2-FC, catalyzed by (*Si*)-CS, is a potent inhibitor of aconitase (20). Thus, if the putative CS does not catalyze the formation of (−)-*erythro*-2-FC but a different 2-FC isomer, then the toxicity of FAc is not expected to be observed for *H. modesticaldum*. This hypothesis is further elaborated below.

Different Isomers of 2-FC Produced by (Re)- Versus (Si)-CS

Although there is no difference in the stereochemistry of citrate from condensation of acetyl-CoA and OAA catalyzed by (*Si*)-CS *versus* (*Re*)-CS (Fig. 3), different isomers of 2-F-citrate (2-FC) are produced from condensation of F-acetyl-CoA and OAA catalyzed by (*Si*)-CS *versus* (*Re*)-CS (Fig. 5). Lauble *et al.* (20) proposed that interactions of (−)-*erythro*-2-FC with aconitase produce an intermediate that inhibits aconitase, whereas interactions of (+)-*erythro*-2-FC with aconitase leads to formation of α-KG, instead of inhibiting aconitase.

To test this hypothesis, we performed physiological studies with the sulfate-reducing bacterium *D. vulgaris* Hildenborough (DvH) using FAc. Acetate can serve as a carbon source for DvH in the presence of reducing power, which can be generated during lactate-supported growth (supplemental Table S2). Thus, FAc, like acetate, can be assimilated by DvH using the reducing power generated by lactate oxidation. Like *H. modesticaldum*, no genes encoding ACL and (*Si*)-CS have been annotated in the DvH genome, whereas the activity of (*Re*)-CS and contribution of CS to the carbon flow of the OTCA cycle have been identified for DvH (24). Fig. 2*C* shows no inhibition for the

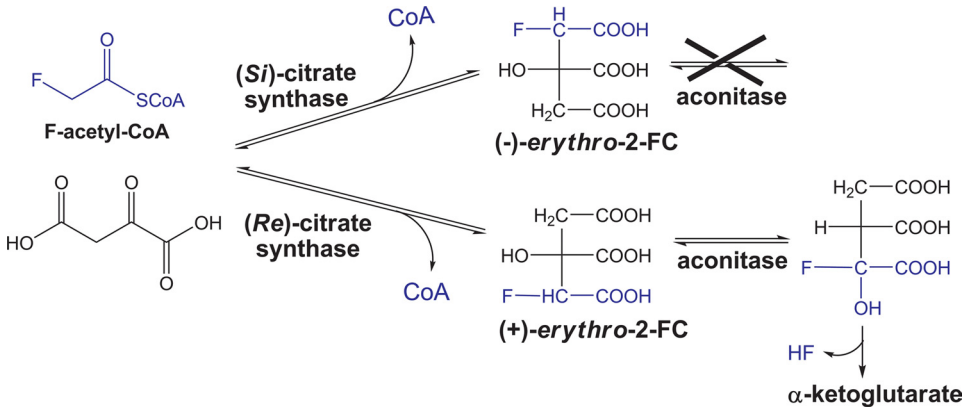

FIGURE 5. **Reaction of F-acetyl-CoA and OAA catalyzed by (*Re*)- *versus* (*Si*)-citrate synthase, and interactions of (−)-*erythro*-2-FC *versus* (+)-*erythro*-2-FC with aconitase.**

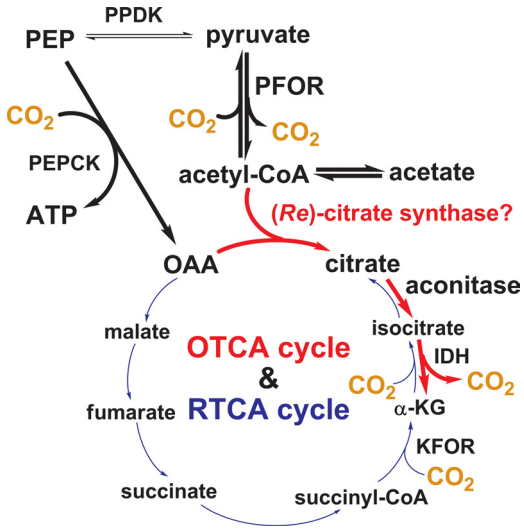

FIGURE 6. **New view for carbon flow in *H. modesticaldum*.** The proposed carbon flow is through the OTCA cycle (*red*) and the RTCA cycle (*blue*) with a stronger flux through the OTCA cycle (acetyl-CoA → α-KG, shown in *bold*). The proposed role of the putative (*Re*)-citrate synthase is shown.

growth of DvH with FAc, consistent with the hypothesis by Lauble *et al.* (20). Consequently, we believe that the lack of FAc inhibition on the growth of *H. modesticaldum* is in agreement with generation of (+)-*erythro*-2-FC, instead of (−)-*erythro*-2-FC, by (*Re*)-CS.

Homocitrate Synthase May Function as (Re)-CS in H. modesticaldum

(*Re*)-CS has been identified in *Clostridium kluyveri* (19), AND THE ACTIVITY OF (*Re*)-CS has been reported in *Thermoanaerobacter* sp. X514 (22), DvH (24), *Dehalococcoides ethenogenes* 195 (26), *Ignicoccus hospitalis* (27), and several anaerobic bacteria. Because different stereoisomers of citrates are generated through the catalysis of (*Re*)- *versus* (*Si*)-CS, it is not surprising that these two types of CS are rather phylogenetically distinct (19, 28).

As mentioned under "Results," the product turnover catalyzed by an oxygen-sensitive CS, possibly a putative (*Re*)-CS, has been detected with Mn^{2+} ions supplied while minimizing oxygen content in the assay solution. Although the gene encoding (*Re*)-CS has not been annotated in the *H. modesticaldum* genome, homocitrate synthase has been suggested to be phylogenetically related to (*Re*)-CS (19). It is possible that homocitrate synthase catalyzes not only the formation of homocitrate from acetyl-CoA and α-KG but also the formation of citrate from acetyl-CoA and OAA (*i.e.* (*Re*)-CS). Two genes in the *H. modesticaldum* genome possibly encode homocitrate synthase, *nifV* (HM1_0858) and *aksA* (HM1_2993). A BLAST search shows that proteins encoded by both genes, particularly by *askA*, share high identity with the reported putative homocitrate synthase/(*Re*)-CS, in agreement with the observed higher transcript level (*i.e.* lower ΔC_T) of *askA* compared with that of *nifV* (Table 1). Given the data presented in this study, we propose that the putative homocitrate synthase, an enzyme that has been reported to function as (*Re*)-CS in several bacteria, is likely responsible for synthesizing citrate in *H. modesticaldum*.

New View for Carbon Flow of H. modesticaldum

Fig. 6 represents a new model for the carbon flow of *H. modesticaldum* that reflects improved understanding resulting from isotopomer and activity assays; the major carbon flux of *H. modesticaldum* is through the OTCA cycle. (*Re*)-citrate synthase, identified in several *Clostridia* and other anaerobic bacteria, is likely employed by *H. modesticaldum* to produce citrate for entering the OTCA cycle. The finding of the OTCA cycle herein fills the knowledge gap for the carbon flow of *H. modesticaldum*. It is intriguing to learn that the major carbon flux of *H. modesticaldum* is switched from the RTCA cycle to the OTCA cycle when the only gene (ATP citrate lyase) missing in the RTCA cycle is replaced by a gene with novel function ((*Re*)-citrate synthase) in the OTCA cycle. Together, our studies suggest that the carbon flow of *H. modesticaldum* (and perhaps *Heliobacterium* strain HY-3) is more akin to *Clostridia* than to the green sulfur bacteria, which employ the RTCA cycle for CO_2 assimilation and biomass production (25).

REFERENCES

1. Madigan, M. T. (2006) *Prokaryotes* **4,** 951–964
2. Asao, M., and Madigan, M. T. (2010) *Photosynth. Res.* **104,** 103–111
3. Kimble, L. K., Mandelco, L., Woese, C. R., and Madigan, M. T. (1995) *Arch. Microbiol.* **163,** 259–267
4. Tang, K. H., Yue, H., and Blankenship, R. E. (2010) *BMC Microbiol.* **10,** 150
5. Sattley, W. M., Madigan, M. T., Swingley, W. D., Cheung, P. C., Clocksin, K. M., Conrad, A. L., Dejesa, L. C., Honchak, B. M., Jung, D. O., Karbach, L. E., Kurdoglu, A., Lahiri, S., Mastrian, S. D., Page, L. E., Taylor, H. L., Wang, Z. T., Raymond, J., Chen, M., Blankenship, R. E., and Touchman, J. W. (2008) *J. Bacteriol.* **190,** 4687–4696
6. Heinnickel, M., and Golbeck, J. H. (2007) *Photosynth. Res.* **92,** 35–53
7. Baymann, F., and Nitschke, W. (2010) *Photosynth. Res.* **104,** 177–187
8. Golbeck, J. H. (2010) *Photosynth. Res.* **104,** 101–102
9. Pickett, M. W., Williamson, M. P., and Kelly, D. J. (1994) *Photosynth. Res.* **41,** 75–88
10. Tang, Y. J., Hwang, J. S., Wemmer, D. E., and Keasling, J. D. (2007) *Appl. Environ. Microbiol.* **73,** 718–729
11. Overmann, J. (2006) *Prokaryotes* **7,** 359–378

12. Tang, K. H., Feng, X., Tang, Y. J., and Blankenship, R. E. (2009) *PLoS One.* **4,** e7233
13. Widdel, F., and Pfennig, N. (1984) in *Bergey's Manual of Systematic Bacteriology* (Krieg, N. R., and Holt, J. G., eds) Vol. 1, pp. 663–679, Williams & Wilkins, Baltimore
14. Brysch, K., Schneider, C., Fuchs, G., and Widdel, F. (1987) *Arch. Microbiol.* **148,** 264–274
15. Wolin, E. A., Wolin, M. J., and Wolfe, R. S. (1963) *J. Biol. Chem.* **238,** 2882–2886
16. Tang, K. H., Wen, J., Li, X., and Blankenship, R. E. (2009) *J. Bacteriol.* **191,** 3580–3587
17. Wahl, S. A., Dauner, M., and Wiechert, W. (2004) *Biotechnol. Bioeng.* **85,** 259–268
18. Bradford, M. M. (1976) *Anal. Biochem.* **72,** 248–254
19. Li, F., Hagemeier, C. H., Seedorf, H., Gottschalk, G., and Thauer, R. K. (2007) *J. Bacteriol.* **189,** 4299–4304
20. Lauble, H., Kennedy, M. C., Emptage, M. H., Beinert, H., and Stout, C. D. (1996) *Proc. Natl. Acad. Sci. U.S.A.* **93,** 13699–13703
21. Tang, Y., Pingitore, F., Mukhopadhyay, A., Phan, R., Hazen, T. C., and Keasling, J. D. (2007) *J. Bacteriol.* **189,** 940–949
22. Feng, X., Mouttaki, H., Lin, L., Huang, R., Wu, B., Hemme, C. L., He, Z., Zhang, B., Hicks, L. M., Xu, J., Zhou, J., and Tang, Y. J. (2009) *Appl. Environ. Microbiol.* **75,** 5001–5008
23. Marcus, A., and Elliott, W. B. (1956) *J. Biol. Chem.* **218,** 823–830
24. Pingitore, F., Tang, Y., Kruppa, G. H., and Keasling, J. D. (2007) *Anal. Chem.* **79,** 2483–2490
25. Tang, K. H., and Blankenship, R. E. (July 22, 2010) *J. Biol. Chem.* 10.1074/jbc.M110.157834
26. Tang, Y. J., Yi, S., Zhuang, W. Q., Zinder, S. H., Keasling, J. D., and Alvarez-Cohen, L. (2009) *J. Bacteriol.* **191,** 5224–5231
27. Jahn, U., Huber, H., Eisenreich, W., Hügler, M., and Fuchs, G. (2007) *J. Bacteriol.* **189,** 4108–4119
28. Lamzin, V. S., Dauter, Z., and Wilson, K. S. (1995) *Curr. Opin. Struct. Biol.* **5,** 830–836

Supporting Information

Isotopomer analysis. Cell pellets were hydrolyzed in 6 M HCl at 100°C for 24 hrs. After air-drying overnight, the dried samples containing free amino acids were derivatized with *N*-(tert-butyl-dimethylsilyl)-*N*-methyl-trifluoroacetamide in tetrahydrofuran at 70°C for 1 hr. Isotopomer measurements were made on a GC (Hewlett-Packard, model 6890, Agilent Technologies, Palo Alto, CA) equipped with a DB5-MS column (J&W Scientific, Falsom, CA) and a mass spectrometer (MS) (5975, Agilent Technologies, Palo Alto, CA). Several groups of charged fragments were detected by GC-MS for the amino acids: the $[M-57]^+$ or $[M-15]^+$ group, which contains un-fragmented amino acids; the $[M-159]^+$ or $[M-85]^+$ group, which contains amino acids losing α carboxyl group; and the f302 group, which contains the fragments of the first two carbons from derivatized amino acids. The $[M-57]^+$ peaks in leucine and isoleucine overlap with other peaks. Published algorithms were used to correct the effects of natural isotopes on the mass distributions of amino acids (1) mass fractions (i.e. M0, M1, M2… which are fractions of unlabeled, single-labeled, and double-labeled amino acids...).

Table S1. Sequences of primers described in this report.

Gene (loci number, predicted/ reported function)	Forward primer (5'→ 3')	Reverse primer (5'→ 3')
16S rRNA gene	GCAACGCGAAGAACCTTACC	GGGCACCCTCGCATCTC
pykA (HM1_0076, pyruvate kinase)	GCCCGAATCATCTCCATCAG	AACGCCCCGCACGAA
acn (HM1_0105, aconitase)	AATCAGCCTGTGGTCCCTGT	CAGAGACACCGCCCGAGTT
fdxR (HM1_0289, ferredoxin-$NADP^+$ reductase, FNR)	CCTGCTCCCGGTCAAAATC	TTCTTCGCGCCGATGAA
porA (HM1_0807, pyruvate: Fd oxidoreductase, PFOR)	GAAGCCTGCAACCCCTACTATAAG	GGTGAGTTTGCCGATCTCCTT
acsA (HM1_0951, acetyl-CoA synthetase)	TCCAAACCTGAAATCCTATGAAGAG	AGAACTCGCGCTCCACATCT
icd (HM1_1471, isocitrate dehydrogenase)	TCAACCCCGGATCGGTC	CTGCCAGCCGAGGTGTTC
mdh (HM1_1472, malate dehydrogenase	CGGCTATGAGGGCATCTACAC	CGGTCAGCTCGATCTCAAAGA
ackA (HM1_2157, acetate kinase)	CCCGCGTCGGTGACAT	CGTCAATCCCTCTTTTTCCATC
ppdK (HM1_2461, pyruvate phosphate dikinase)	AGATGTCGTTGCCGGTATCC	AAGCATTCGGGCAGTTCTTC
korC (HM1_2762, KFOR, γ subunit)	GGGAAGCCCTCGAAAAAGC	TGTTCATCTCCTCGGTCCCT
oorB (HM1_2763, KFOR, β subunit)	AAAGGGACCACCGCTCCT	GCCAGGTTGCAGATGTCGA
korA (HM1_2766, KFOR, α subunit)	CGGCGACCATCCTGTCAT	CCGTCAGGTTGAAGCATTCC
korD (HM1_2767, KFOR, δ subunit)	AAGTGTTGGGCGCTGACG	TGCACTTGGTACATTTTTTCGG
nifV (HM1_0858, homocitrate synthase)	GAAGCCTATCCGCCCGA	GCTGTATTTGCCAAAGGCGA
aksA (HM1_2993, homocitrate synthase)	CGCTTCCCGTTCTGATATTGA	CGCCCAGCTTTTTGGCTT
pckA (HM1_2773, PEP carboxykinase)	GATGCCATCTTCCACGAGGTA	CAGTCCCTGTTACGTGTCGAAA

Table S2. Isotopomer labeling patterns of protein-based amino acids in the *Desulfovibrio vulgaris* Hildenborough (DvH) cultures grown on non-labeled lactate and [2-^{13}C]acetate.[a]

Amino acid	Precursor	Ion	M-57	M-159
Ala	pyruvate	M0	0.89	0.85
		M1	**0.10**	**0.12**
		M2	**0.01**	**0.03**
Leu	pyruvate acetyl-CoA	M0		0.34
		M1	peaks	**0.49**
		M2	overlapped	**0.14**
Phe	phosphoenolpyruvate erythrose-4-phosphate	M0	0.65	0.63
		M1	**0.28**	**0.29**
		M2	**0.05**	**0.06**
Asp	oxaloacetate	M0	0.85	0.86
		M1	**0.14**	**0.10**
		M2	**0.01**	**0.02**
Glu	α-ketoglutarate	M0	0.43	0.42
		M1	**0.49**	**0.50**
		M2	**0.03**	**0.06**
His	ribose-5-phosphate	M0	0.78	0.81
		M1	**0.13**	**0.13**
		M2	**0.06**	**0.03**

[a] While DvH cannot grow using acetate as the sole carbon and energy source, DvH can grow with a mixed-substrate (lactate and acetate). When [2-^{13}C]acetate and non-labeled lactate with 1:1 molar ratio were presented in DvH growth medium, a doubling time ~ 9 hours was observed during the middle-log phase. The labeling carbons were significantly enriched in its protein-based amino acids for the cultures harvested during the late-log growth phase (see Table above), indicating that labeled acetate was partially utilized for protein synthesis in the mixed-substrate culture. The labeling data presented above also illustrates that acetate ↔ acetyl-CoA ↔ pyruvate is a reversible pathway. The DvH culture condition was described in the Experimental Procedures.

Table S3. Isotopomer labeling patterns of protein-based amino acids in the *H. modesticaldum* cultures grown on [3-^{13}C]pyruvate.

Amino acid	Precursor	Ion	M-57	M-159	f302	Proposed 13C enriched positions
Ala	pyruvate	M0	0.06	0.09	0.13	*C-C-COOH
		M1	0.89	0.80	0.85	
		M2	0.05	0.11	0.02	
Gly	serine	M0	0.70	0.72	0.28	*C-COOH
		M1	0.29	0.28	0.35	
		M2	0.01		0.37	
Val	pyruvate	M0	0.06	0.08	0.73	*C-*C-C-C-COOH
		M1	0.03	0.05	0.18	
		M2	0.87	0.78	0.10	
Leu	pyruvate	M0	0.06	0.08	0.28	*C-*C-C-C-*C-COOH
	acetyl-CoA	M1	0.02	0.02	0.30	
		M2	0.15	0.27	0.42	
		M3	0.75	0.57		
Ile	pyruvate	M0	0.05	0.05	0.22	*C-*C-C-C-*C-COOH
	threonine	M1	0.02	0.02	0.48	
		M2	0.27	0.34	0.29	
		M3	0.64	0.57		
Met	aspartate	M0	0.06	0.06	0.29	*C-S-C-*C-C-COOH
	methyl-THF	M1	0.37	0.39	0.54	
		M2	0.52	0.52	0.17	
		M3	0.05	0.04		
Ser	3-phospho-	M0	0.09	0.09	0.75	*C-C-COOH
	glycerate	M1	0.87	0.89	0.24	
		M2	0.04	0.02	0.01	
Thr	aspartate	M0	0.07	0.08	0.11	C-*C-C-COOH
		M1	0.83	0.86	0.64	
		M2	0.11	0.07	0.25	
Phe	PEP	M0	0.06	0.06	0.76	*C-*C-C-C-C-C-*C-C-COOH (clockwise)
	erythrose-4-	M1	0.01	0.01	0.23	
	phosphate	M2	0.04	0.05	0.01	
		M3	0.74	0.75		
		M4	0.14	0.13		
Asp	OAA	M0	0.06	0.06	0.58	C-*C-C-COOH
		M1	0.82	0.87	0.39	
		M2	0.12	0.07	0.03	

Glu	α-KG	M0	0.07	0.07	0.71	C-*C-C-*C-COOH
		M1	0.10	0.22	0.24	
		M2	0.76	0.67	0.05	
		M3	0.07	0.05		
His	ribose-5-	M0	0.06	0.13	0.14	N-*C-N-C-C-C-C-*COOH
	phosphate	M1	0.12	0.43	0.78	
		M2	0.53	0.35	0.08	
		M3	0.28	0.08		
Lys	aspartate	M0	0.07	0.07	0.91	C-*C-C-*C-C-COOH
	pyruvate	M1	0.05	0.04	0.09	
		M2	0.79	0.81	0.00	
		M3	0.09	0.06		
		M4	0.00	0.01		

Table S4. Isotopomer labeling patterns of protein-based amino acids in the *H. modesticaldum* cultures grown on ^{13}C-labeled sodium bicarbonate and non-labeled pyruvate.

Amino acid	Precursors	Ions	M-57	M-159	f302	Proposed 13C enriched positions
Ala	pyruvate	M0	0.47	0.92	0.47	C-C-*COOH
		M1	0.52	0.03	0.53	
		M2	0.01	0.05	0.00	
Gly	serine	M0	0.49	0.99	0.24	C-*COOH
		M1	0.51	0.01	0.29	
		M2	0.01		0.47	
Val	pyruvate	M0	0.43	0.93	0.51	C-C-C-C-*COOH
		M1	0.54	0.05	0.48	
		M2	0.03	0.01	0.01	
Leu	pyruvate	M0	0.74	0.92	0.80	Non-labeled
	acetyl-CoA	M1	0.20	0.07	0.19	
		M2	0.02	0.01	0.01	
		M3	0.04	0.00		
Ile	pyruvate	M0	0.64	0.86	0.65	Non-labeled
	threonine	M1	0.29	0.13	0.31	
		M2	0.07	0.01	0.04	
		M3	0.00	0.00		
Met	aspartate	M0	0.23	0.42	0.28	C-S-*C-C-C-*COOH
	methyl-THF	M1	0.45	0.52	0.42	
		M2	0.29	0.04	0.30	
		M3	0.03	0.01		
Ser	3-phospho-	M0	0.45	0.96	0.48	C-C-*COOH
	glycerate	M1	0.54	0.03	0.51	
		M2	0.02	0.01	0.01	
Thr	aspartate	M0	0.23	0.43	0.20	*C-C-C-*COOH
		M1	0.47	0.57	0.49	
		M2	0.30	0.02	0.31	
Phe	PEP	M0	0.14	0.27	0.41	C-C-*C-*C-C-C-C-C-*COOH
	erythrose-4-	M1	0.32	0.45	0.59	
	phosphate	M2	0.35	0.25	0.00	
		M3	0.18	0.03		
		M4	0.01	0.00		
Asp	OAA	M0	0.24	0.47	0.47	*COOH-C-C-*COOH
		M1	0.46	0.52	0.53	
		M2	0.31	0.01	0.00	
Glu	α-KG	M0	0.38	0.43	0.78	C-C-C-C-*COOH

		M1	0.50	0.54	0.21	
		M2	0.11	0.02	0.01	
		M3	0.00	0.00		
Lys	aspartate	M0	0.26	0.42	0.87	C-C-*C-C-C-*COOH
	Pyruvate	M1	0.41	0.54	0.13	
		M2	0.34	0.03	0.00	
		M3	0.00	0.01		
		M4	0.01	0.00		

Table S5. List of bacteria with the citramalate pathway reported.

Species	References	CimA similarity (GSU1798)	CimA similarity (MJ1392)	Growth conditions
Roseobacter denitrifican	(2)	RD1_3182, 45%	RD1_1121, 40%	aerobic
Methanobacterium thermoautotrophicum	(3)	MTH1481, 28%	MTH723, 58%	anaerobic
Methanococcus jannaschii	(4)	ND	MJ1392, 100%	aerobic (*E. coli*)
Leptospira interrogans	(5,6), (7)	LIC11726, 26%	LIC11726, 41%	aerobic (*E. coli*)
Thermoproteus neutropkilccs	(8)	Tneu_0320, 45%	Tneu_0832, 55%	anaerobic, thermophilic
Ignicoccus hospitalis	(9)	Igni_0645, 45%	Igni_0983, 52%	anaerobic, thermophilic
Geobacter sulfurreducens	(10)	GSU1798, 100%	GSU1906, 41%	anaerobic
Geobacter metallireducens	(11)	Gmet_1879, 92%	Gmet_1265, 42%	anaerobic
Serratia marcescens	(12)	Spro_0745, 26%	Spro_0745, 37%	anaerobic
Thermoanaerobacter sp. X514	(13)	Teth514_1204 49%	Teth514_0415 45%	anaerobic, thermophilic
Dehalococcoides ethenogenes 195	(14)	DET0825, 53%	DET0830, 41%	anaerobic
Heliobacterium modesticaldum	(15) and this report	HM_1519, 55%	HM_1515, 45%	anaerobic

Fig. S1. The normal versus the novel pathway for lysine biosynthesis in the *H. modesticaldum* cultures grown on [1-^{13}C]pyruvate. Predicted labeled carbons are marked by asterisks.

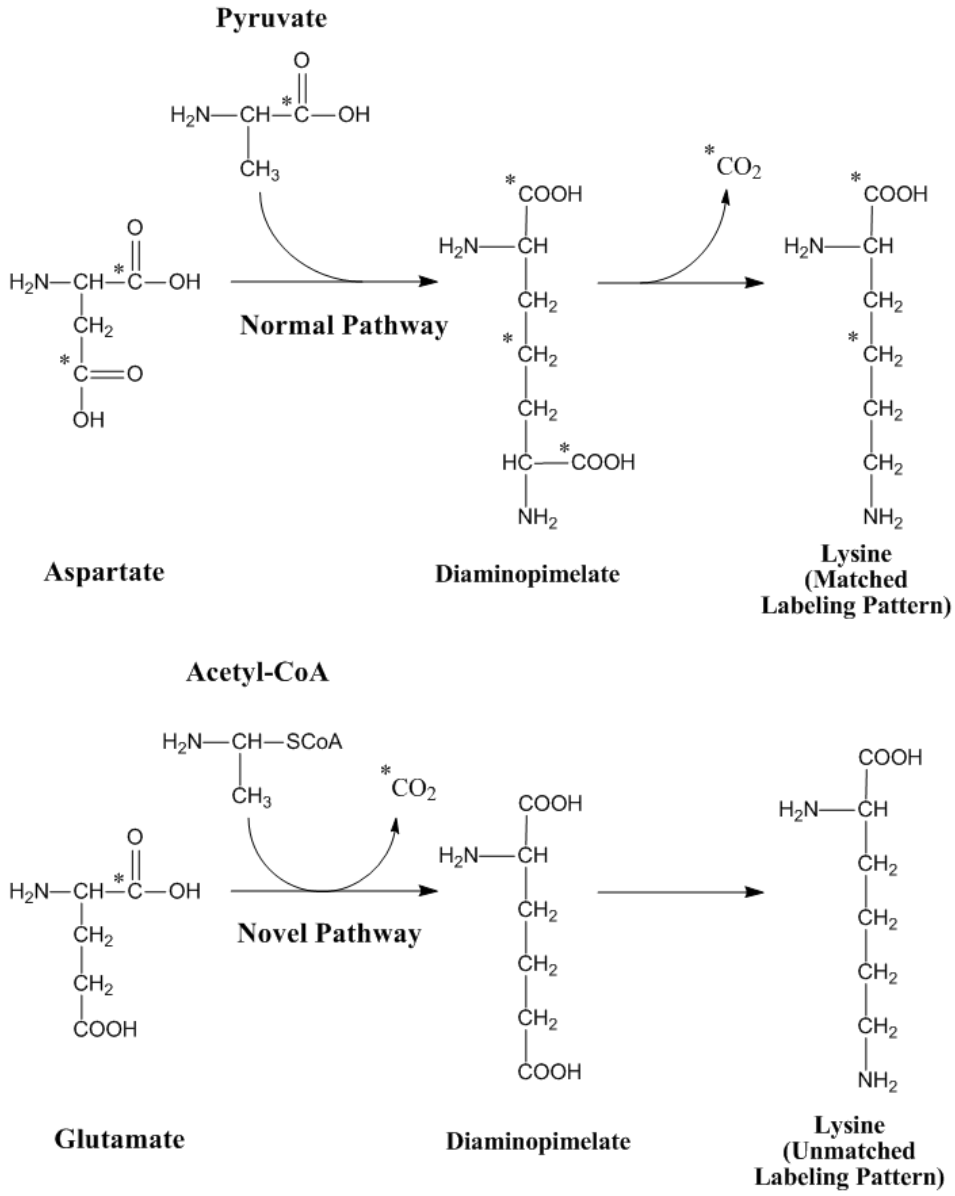

References in Supporting Information

1. Wahl, S. A., Dauner, M., and Wiechert, W. (2004) *Biotechnol. Bioeng.* **85**(3), 259-268
2. Tang, K. H., Feng, X., Tang, Y. J., and Blankenship, R. E. (2009) *PLoS One* **4**(10), e7233
3. Eikmanns, B., Linder, D., and Thauer, R. K. (1983) *Arch. Microbiol.* **136**(2), 111-113
4. Howell, D. M., Xu, H. M., and White, R. H. (1999) *J. Bacteriol.* **181**(1), 331-333
5. Charon, N. W., Johnson, R. C., and Peterson, D. (1974) *J Bacteriol* **117**(1), 203-211
6. Westfall, H. N., Charon, N. W., and Peterson, D. E. (1983) *J. Bacteriol* **154**(2), 846-853
7. Xu, H., Zhang, Y. Z., Guo, X. K., Ren, S. X., Staempfli, A. A., Chiao, J. S., Jiang, W. H., and Zhao, G. P. (2004) *J. Bacteriol.* **186**(16), 5400-5409
8. Schäfer, S., Paalme, T., Vilu, R., and Fuchs, G. (1989) *Eur J Biochem* **186**, 695-700
9. Jahn, U., Huber, H., Eisenreich, W., Hugler, M., and Fuchs, G. (2007) *J. Bacteriol.* **189**(11), 4108-4119
10. Risso, C., Van Dien, S. J., Orloff, A., Lovley, D. R., and Coppi, M. V. (2008) *J. Bacteriol.* **190**(7), 2266-2274
11. Tang, Y. J., Chakraborty, R., Martin, H. G., Chu, J., Hazen, T. C., and Keasling, J. D. (2007) *Appl. Environ. Microbiol.* **73**(12), 3859-3864
12. Kisumi, M., Komatsubara, S., and Chibata, I. (1977) *J. Biochem.* **82**(1), 95-103
13. Feng, X., Mouttaki, H., Lin, L., Huang, R., Wu, B., Hemme, C. L., He, Z., Zhang, B., Hicks, L. M., Xu, J., Zhou, J., and Tang, Y. J. (2009) *Appl. Environ. Microbiol.* **75**(15), 5001-5008
14. Tang, Y. J., Yi, S., Zhuang, W. Q., Zinder, S. H., Keasling, J. D., and Alvarez-Cohen, L. (2009) *J. Bacteriol.* **191**(16), 5224-5231
15. Pickett, M. W., Williamson, M. P., and Kelly, D. J. (1994) *Photosynth. Res.* **41**, 75-88